Ab initio Calculation of the Intrinsic Spin Hall Effect in Semiconductors

G. Y. Guo,[1,*] Yugui Yao,[2] and Qian Niu[3]

[1]*Department of Physics, National Taiwan University, Taipei 106, Taiwan*
[2]*Institute of Physics, Chinese Academy of Sciences, Beijing 100080, China*
[3]*Department of Physics, University of Texas at Austin, Austin, Texas 78712-1081, USA*

(Received 12 November 2004; published 8 June 2005)

Relativistic band theoretical calculations reveal that intrinsic spin Hall conductivity in hole-doped archetypical semiconductors Ge, GaAs, and AlAs is large [$\sim 100(\hbar/e)(\Omega\,\mathrm{cm})^{-1}$], showing the possibility of a spin Hall effect beyond the four-band Luttinger Hamiltonian. The calculated orbital-angular-momentum (orbital) Hall conductivity is one order of magnitude smaller, indicating no cancellation between the spin and orbital Hall effects in bulk semiconductors. Furthermore, it is found that the spin Hall effect can be strongly manipulated by strains, and that the ac spin Hall conductivity is large in pure as well as doped semiconductors.

DOI: 10.1103/PhysRevLett.94.226601 PACS numbers: 72.25.Dc, 71.20.−b, 72.20.−i, 85.75.−d

Spin-orbit coupling is known to be responsible for a whole range of interesting phenomena in magnetic materials [1], including magnetic anisotropy, optical dichroism, and anomalous Hall effect. Spin generation and transport in paramagnetic materials can also be induced by an electric field because of spin-orbit coupling even in the absence of a magnetic field as demonstrated in a number of recent experiments [2]. This offers the exciting possibility of pure electric driven spintronics in semiconductors, where spin-orbit coupling is relatively strong and which can be more readily integrated with conventional electronics [3]. Earlier theories on electric spin generation and transport were based on extrinsic effects due to spin-orbit coupling in scattering processes [4]. Recently, it has been proposed that a transverse spin current response to an electric field, known as the intrinsic spin Hall effect, can also occur in pure crystalline materials due to intrinsic spin-orbit coupling in the band structure [5,6].

A large number of theoretical papers have been written addressing various issues about the intrinsic spin Hall effect. In [7], a systematic semiclassical theory of spin transport is presented, resolving a discrepancy between the prediction of [5] and the Kubo formula result. In [8], an orbital-angular-momentum (orbital) Hall current is predicted to exist in response to an electric field and is found to cancel exactly the spin Hall current in the spin Hall effect. There is also an intensive debate about whether the intrinsic spin Hall effect remains valid beyond the ballistic transport regime [9]. On the other hand, experimental measurements of large spin Hall effects for the Rashba two-dimensional electron gas and for n-type bulk semiconductors have just been reported [10,11], although more work is needed to firmly establish the intrinsic or extrinsic nature of the results. It is expected that similar experiments on p-type semiconductors will also appear soon.

Inspired by the prospect that the intrinsic spin Hall effect may provide a useful property for spintronics applications which is designable based on material parameters, we have carried out *ab initio* calculations on this effect and related phenomena in the archetypical p-type semiconductors Si, Ge, GaAs, and AlAs. We focus on the p-type because the spin-orbit coupling is much stronger in the valence bands, where the intrinsic effect has a better chance of dominating over the extrinsic scattering effects. Such results are clearly needed to provide a stage for systematic and quantitative comparison between theoretical predictions and experimental measurements. In addition, the calculations may also help resolve some of the theoretical issues for such semiconductors whose discussions are currently all based on the four-band Luttinger Hamiltonian for the holes and often with the spherical approximation.

Our results cover a large range of hole concentration which is beyond the validity regime of the four-band model. By including all the relevant bands, we find a pronounced spin Hall conductivity for all the semiconductors except the light element Si and a roughly quadratic dependence of the spin Hall conductivity on the spin-orbit gap. The vanishing of spin Hall conductivity in the limit of zero spin-orbit coupling differs qualitatively with the prediction of the four-band model, which yields a finite spin Hall conductivity even when spin-orbit coupled terms in the Luttinger Hamiltonian approach zero [5,12]. We also calculated the orbital Hall effect, and find it an order of magnitude weaker than the spin Hall effect, a result due to the orbital quenching by the cubic anisotropy of the crystals. This is in sharp contrast to the case of the Rashba two-dimensional electron system and the spherical four-band model, where exact cancellation between the spin and orbital Hall effects occurs due to rotational symmetry in such models [8]. In addition, we calculated the effect of strain, which is commonly present in semiconductor multilayers and superlattices due to lattice mismatch, and which may be used to enhance or reduce the spin Hall effect. Furthermore, this result on strain effect will help the experimentalists to distinguish intrinsic from extrinsic aspect of the spin Hall effect in the future [11]. Finally, we also

calculated the ac spin Hall conductivity and find it to be large in both pure and hole-doped semiconductors.

The intrinsic Hall conductivity of a solid can be evaluated by using the Kubo formula approach [13]. In this approach, the intrinsic Hall effect comes from the static $\omega = 0$ limit of the off-diagonal element of the conductivity tensor [6,13]:

$$\sigma_{xy}(\omega) = \frac{e}{i\omega V_c}\sum_{\mathbf{k}}\sum_{n\neq n'}(f_{\mathbf{k}n} - f_{\mathbf{k}n'}) \times \frac{\langle \mathbf{k}n|j_x|\mathbf{k}n'\rangle\langle \mathbf{k}n'|v_y|\mathbf{k}n\rangle}{\epsilon_{\mathbf{k}n} - \epsilon_{\mathbf{k}n'} + \hbar\omega + i\eta} \quad (1)$$

where V_c is the unit cell volume, $\hbar\omega$ is the photon energy, and $|\mathbf{k}n\rangle$ is the nth Bloch state with crystal momentum $\mathbf{k}$. Since all the intrinsic Hall effects are caused by spin-orbit coupling, first-principles calculations must be based on a relativistic band theory. In this case, the current operators $\mathbf{j}$ are $-e\mathbf{v}$, $\frac{\hbar}{4}\{\beta\Sigma_z, \mathbf{v}\}$, and $\frac{\hbar}{2}\{\beta L_z, \mathbf{v}\}$ for the anomalous, spin, and orbital Hall effects, respectively. Here β, Σ are the well-known 4×4 Dirac matrices [14], and $\mathbf{v}$ is the velocity operator projected onto states above the electron-positron mass gap [15]. Setting η to zero and using $\mathrm{Im}[1/(x - i\eta)] = \pi\delta(x)$, one obtains the imaginary part of the off-diagonal element

$$\sigma''_{xy}(\omega) = -\frac{\pi e}{\omega V_c}\sum_{\mathbf{k}}\sum_{n\neq n'}(f_{\mathbf{k}n} - f_{\mathbf{k}n'})\mathrm{Im}[\langle \mathbf{k}n|j_x|\mathbf{k}n'\rangle \times \langle \mathbf{k}n'|v_y|\mathbf{k}n\rangle]\delta(\epsilon_{n'n} - \hbar\omega) \quad (2)$$

where $\epsilon_{n'n} = \epsilon_{\mathbf{k}n'} - \epsilon_{\mathbf{k}n}$. As in previous magneto-optical calculations [15], we first calculate the imaginary part of the σ_{xy} and then obtain the real part from the imaginary part by a Kramers-Kronig transformation

$$\sigma'_{xy}(\omega) = \frac{2}{\pi}\mathbf{P}\int_0^\infty d\omega' \frac{\omega'\sigma''_{xy}(\omega')}{\omega'^2 - \omega^2} \quad (3)$$

where $\mathbf{P}$ denotes the principal value of the integral. We notice that the anomalous Hall conductivity $\sigma_{xy}(0)$ of bcc Fe calculated this way [15,16] is in good quantitative agreement with that calculated directly by a generalized Boltzmann equation approach that accounts for the Berry phase correction to the group velocity [16].

TABLE I. Experimental lattice constant a (see [20] and references therein), average atomic sphere radius R_{ws} and band gap E_g (see [21] and references therein) of the semiconductors studied. The calculated band gaps E_g^{the} and spin-orbit splitting Δ_{so} of the top valence bands at Γ are also listed.

	a (Å)	R_{ws} (a.u.)	E_g (eV)	E_g^{the} (eV)	Δ_{so} (meV)
Si	5.431	2.526	1.17	0.81	47
Ge	5.650	2.632	0.74	0.28	278
AlAs	5.620	2.615	2.23	1.52	301
GaAs	5.654	2.632	1.52	0.76	336

The relativistic band structure of the semiconductors is calculated using a fully relativistic extension [17] of the well established all-electron linear muffin-tin orbital method [18]. The calculations are based on density functional theory with generalized gradient approximation (GGA) [19]. In the fcc diamond or zincblend structures, two atoms sit at (0,0,0) and (1/4, 1/4, 1/4), respectively. In the present calculations, two "empty" atomic spheres are introduced at the vacant sites (1/2, 1/2, 1/2) and (3/4, 3/4, 3/4), respectively, to make the structures more close packed. The four "atoms" in the unit cell are assumed to have an equal atomic sphere radius. The experimental lattice constants for Si, Ge, GaAs, and AlAs used are listed in Table I together with the corresponding atomic sphere radii. The basis functions used for all the atoms are s, p, and d muffin-tin orbitals [18]. In the self-consistent electronic structure calculations, eighty-nine k points in the fcc irreducible wedge (IW) of the Brillouin zone (BZ) were used in the tetrahedron BZ integration. The calculated band gaps E_g and spin-orbit splitting Δ_{so} of the top valence bands at Γ for all the semiconductors are listed in Table I. As an example, the calculated band structure of GaAs is displayed in Fig. 1.

In the Hall conductivity calculations, a much finer k-point mesh is needed. Moreover, a larger IW (3 times the fcc IW for Si and Ge, and 6 times the fcc IW for AlAs and GaAs, which have no spatial inversion symmetry) is necessary for the Hall conductivity calculations. The number of k points in the IW used is 49 395 for Si and Ge and 98 790 for GaAs and AlAs. These numbers are obtained by dividing the ΓX line into 56 intervals (see Fig. 1). Test calculations using 139 083 k points (80 divisions of the ΓX line) for Ge indicate that the calculated spin Hall conductivity converge to within 2%. The imaginary part of the

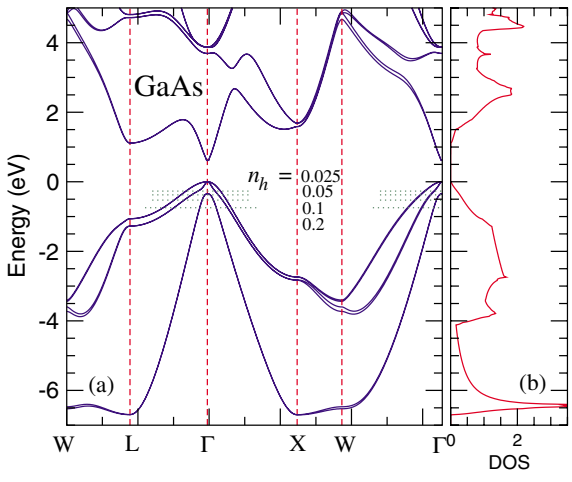

FIG. 1 (color online). Relativistic band structure of GaAs: (a) Energy bands and (b) density of states (DOS) (states/eV/cell). The zero energy is at the top of the valence bands. The dotted lines just below the top of the valence bands denote the Fermi levels for the hole concentration $n_h = 0.025$, 0.05, 0.1, and 0.2 e/cell, respectively.

Hall conductivity is calculated up to 50 eV to ensure that the real part of the conductivity obtained through the Kramers-Kronig transformation converges as well. As is well known, all the calculated band gaps are smaller than the corresponding experimental values though the calculated spin-orbit splittings Δ_{so} agree quite well with the experimental ones as well as the full-potential calculations (see Table I and [22]). To remedy this defect of the GGA, the so-called scissor operator is applied in the conductivity calculations, i.e., all the conduction bands are shifted upwards such that the theoretical band gap is the same as the experimental one.

Figure 2 shows the calculated spin (σ_{xy}^{sH}) and orbital (σ_{xy}^{oH}) Hall conductivities as a function of hole concentration. The spin Hall conductivity in Ge, GaAs, and AlAs increases sharply as the hole concentration n_h increases at small $n_h (n_h \leq 0.02\ e/\text{cell})$ [Fig. 2(a)], being consistent with the recent analytical Luttinger model predictions of $n_h^{1/3}$ [7,23]. However, it becomes more or less flat when n_h is further increased [Fig. 2(a)]. This is due to the fact that the spin Hall effect results predominantly from the spin-orbit split heavy-hole (HH) and light-hole (LH) pockets centered at Γ (Fig. 1) [5]. Figure 1 shows that when $n_h \geq 0.05\ e/\text{cell}$, the Fermi level is already below the top of the lower spin-orbit split valence band. However, there is no substantial increase in the spin Hall conductivity as n_h goes through $0.05\ e/\text{cell}$, indicating that the lower spin-orbit split valence band has no significant contribution to the spin Hall conductivity. Remarkably, the spin conductivity for Ge, GaAs, and AlAs is very pronounced, being about $100\hbar/(e\Omega\ \text{cm})$ (Fig. 2). These values are comparable to the charge conductivity for lightly hole-doped Ge, GaAs, and AlAs, in agreement with the prediction of the large intrinsic spin Hall effect in hole-doped semiconductors based on the Luttinger Hamiltonian [7,23]. However, our results differ from the predictions of the four-band model in at least one important aspect. Figure 2(c) shows that the calculated spin Hall conductivity at, e.g., $n_h = 0.05\ e/\text{cell}$, approaches zero nearly quadratically as the spin-orbit splitting Δ_{so} and hence the spin-orbit coupling strength goes to zero. In contrast, the four-band model yields a finite spin Hall conductivity even as the spin-orbit coupled terms in the Luttinger Hamiltonian approach zero.

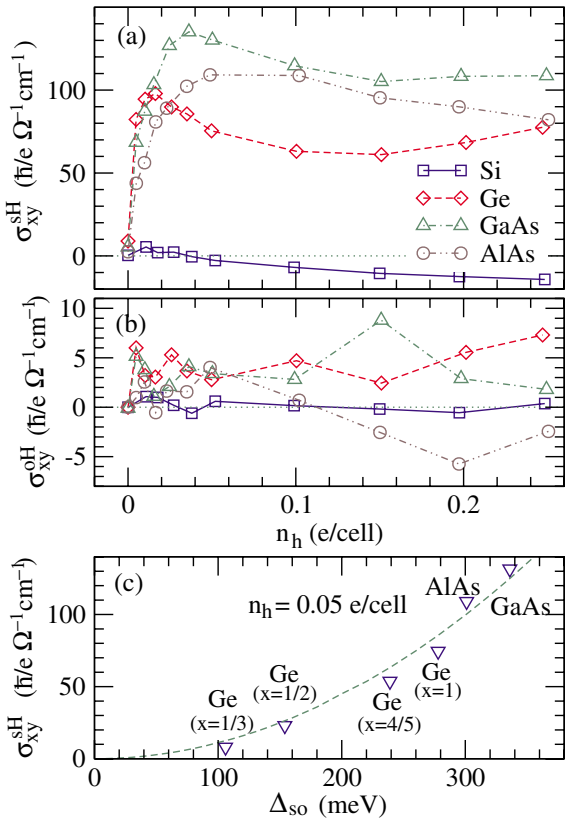

FIG. 2 (color online). Calculated (a) spin (σ_{xy}^{sH}) and (b) orbital (σ_{xy}^{oH}) Hall conductivity as a function of hole concentration (n_h) for Si, Ge, GaAs, and AlAs. (c) Calculated spin Hall conductivity for $n_h = 0.05\ e/\text{cell}$ vs the top valence band spin-orbit splitting (Δ_{so}). The dashed line denotes the parabola fitted to the calculated data. The x is the spin-orbit coupling scaling factor [25]: $x = 1$ means full spin-orbit coupling and $x = 0$ means no spin-orbit coupling. $n_h = 0.1\ e/\text{cell}$ is equivalent to n_h of 2.5×10^{21}, 2.2×10^{21}, 2.2×10^{21}, and $2.3 \times 10^{21}\ \text{cm}^{-3}$ for Si, Ge, GaAs, and AlAs, respectively.

The calculated orbital Hall conductivity is at least 10 times smaller than the spin Hall conductivity (Fig. 2), demonstrating that the orbital Hall effect in bulk semiconductors is strongly quenched by the cubic crystal fields and covalent bonding. Furthermore, the orbital and spin Hall conductivities generally have the same sign when the hole concentration is small, i.e., $n_h \leq 0.1\ e/\text{cell}$ (Fig. 2). Therefore, the exact cancellation of the intrinsic spin Hall effect by the intrinsic orbital Hall effect in the two-dimensional electron gas with the Rashba spin-orbit term predicted in [8] would not occur in bulk semiconductors.

In device applications, semiconductors are typically grown epitaxially on substrates with similar lattice constants, resulting in semiconductor multilayers and superlattices. The semiconductor layers are thus generally strained due to small lattice mismatches. The lattice mis-

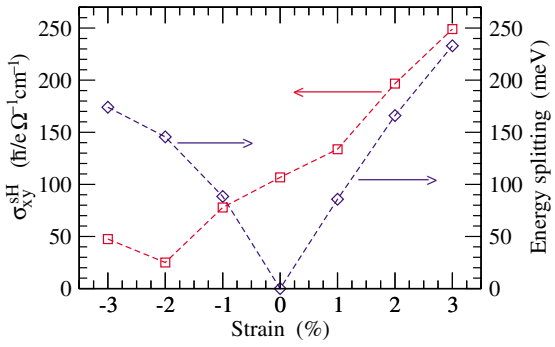

FIG. 3 (color online). Calculated spin Hall conductivity (σ_{xy}^{sH}) (squares) and energy splitting (diamonds) of heavy-hole and light-hole bands at Γ of GaAs as a function of uniaxial strain at the hole concentration $n_h = 0.1\ (e/\text{cell})$.

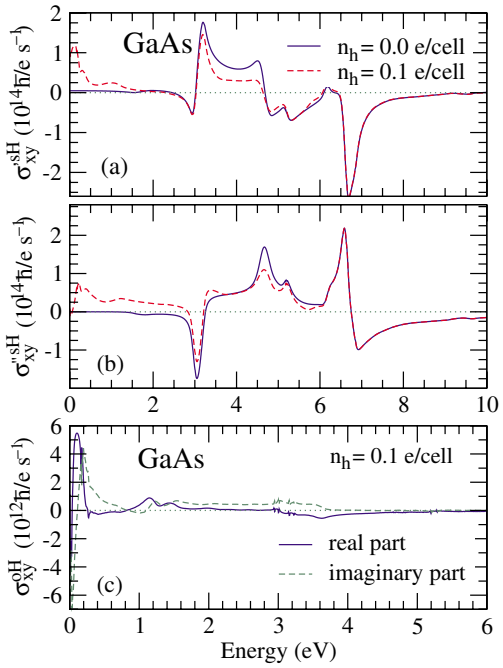

FIG. 4 (color online). Calculated spin (σ_{xy}^{sH}) and orbital (σ_{xy}^{oH}) Hall conductivity of GaAs as a function of frequency at the hole concentrations $n_h = 0.0, 0.1$ (e/cell), respectively.

match strain may have significant effects on the electronic structure of the semiconductors, and hence also on the spin Hall effect [24]. In particular, the degeneracy of the HH and LH bands at Γ would be lifted. We have calculated the band structure and Hall conductivity of GaAs under [001] uniaxial elastic strains. The calculated spin Hall conductivity as well as the energy splitting Δ of the HH and LH bands at Γ are displayed as a function of strain in Fig. 3. Here the strain ε is defined as $a = a_0(1 + \varepsilon)$ where a and a_0 are the strained and unstrained lattice constants perpendicular to [001], respectively. As expected, the Δ is roughly proportional to the strain size. Remarkably, the spin Hall conductivity varies almost linearly with the strain, increasing with tensile change and decreasing with compression in the lateral directions (Fig. 3). This linear and sensitive dependence on the strain may be used to tune the spin Hall effect.

The shape of the calculated ac spin Hall conductivity spectra for all the semiconductors studied here look rather similar, though the peak energy position and peak magnitudes may differ. Thus, we only display in Fig. 4 the ac Hall conductivities for GaAs as a representative. Interestingly, both the real and imaginary parts of the spin Hall conductivity in both pure and hole-doped semiconductors are large [Figs. 4(a) and 4(b)]. This suggests that one could generate ac spin current in semiconductors without using magnetic field or magnetic materials. In contrast, the orbital Hall conductivity in the pure semiconductors is zero (i.e., within numerical noise) while it is 2 orders of magnitude smaller than the spin Hall conductivity in the hole-doped semiconductors (Fig. 4).

The authors thank Ming-Che Chang for stimulating discussions. They thank NCTS/TPE and National Science Council of ROC, NSFC (No. 10404035) of PRC, US Department of Energy (DE-FG03-02ER45958) and the Welch Foundation for financial support, and thank NCHC of ROC for providing CPU time.

*Electronic address: gyguo@phys.ntu.edu.tw

[1] *Spin-orbit Influenced Spectroscopies of Magnetic Solids*, edited by H. Ebert and G. Schütz, Lecture Notes in Physics 466 (Springer-Verlag, Heidelberg, 1996).
[2] Y. Kato *et al.*, Phys. Rev. Lett. **93**, 176601 (2004); Nature (London) **427**, 50 (2004); J. Stephens *et al.*, Phys. Rev. Lett. **93**, 097602 (2004).
[3] S. A. Wolf *et al.*, Science **294**, 1488 (2001).
[4] M. I. Dyakonov and V. I. Perel, Sov. Phys. JETP **33**, 467 (1971); L. S. Levitov *et al.*, Sov. Phys. JETP **61**, 133 (1985); J. E. Hirsch, Phys. Rev. Lett. **83**, 1834 (1999); S. Zhang, Phys. Rev. Lett. **85**, 393 (2000); L. I. Magarill *et al.*, Semiconductors **35**, 1081 (2001).
[5] S. Murakami, N. Nagaosa, and S.-C. Zhang, Science **301**, 1348 (2003).
[6] J. Sinova *et al.*, Phys. Rev. Lett. **92**, 126603 (2004).
[7] D. Culcer *et al.*, Phys. Rev. Lett. **93**, 46602 (2004).
[8] S. Zhang and Z. Yang, Phys. Rev. Lett. **94**, 66602 (2005).
[9] J.-I. Inoue, G. E. W. Bauer, and L. W. Molenkamp, Phys. Rev. B **70**, 041303R (2004); S. Murakami, Phys. Rev. B **69**, 241202R (2004); E. G. Mishchenko, A. V. Shytov, and B. I. Halperin, Phys. Rev. Lett. **93**, 226602 (2004); K. Nomura *et al.*, Phys. Rev. B **71**, 041304 (2005); O. Chalaev and D. Loss, Phys. Rev. B (to be published).A. Khaetskii, cond-mat/0408136; R. Raimondi and P. Schwab, Phys. Rev. B **71**, 033311 (2005).
[10] J. Wunderlich *et al.*, Phys. Rev. Lett. **94**, 47204 (2005).
[11] Y. Kato *et al.*, Science **306**, 1910 (2004).
[12] X. Wang and X.-G. Zhang, J. Magn. Magn. Mater. **288**, 297 (2005).
[13] M. Marder, *Condensed Matter Physics* (John Wiley & Sons, Inc., New York, 2000).
[14] V. B. Berestetskii, E. M. Lifshitz, and L. P. Pitaevskii, *Landau and Lifshitz Course on Theoretical Physics: Relativistic Quantum Theory* (Pergamon Press, Oxford, 1971), Vol. 4.
[15] G. Y. Guo and H. Ebert, Phys. Rev. B **51**, 12633 (1995).
[16] Y. Yao *et al.*, Phys. Rev. Lett. **92**, 37204 (2004).
[17] H. Ebert, Phys. Rev. B **38**, 9390 (1988).
[18] O. K. Andersen, Phys. Rev. B **12**, 3060 (1975).
[19] J. P. Perdew, K. Burke, and M. Ernzerhof, Phys. Rev. Lett. **77**, 3865 (1996).
[20] J. R. Chelikowsky, Phys. Rev. B **35**, 1174 (1987).
[21] K. A. Johnson and N. W. Ashcroft, Phys. Rev. B **58**, 15548 (1998).
[22] P. Carrier and S.-H. Wei, Phys. Rev. B **70**, 35212 (2004).
[23] S. Murakami, N. Nagaosa, and S.-C. Zhang, Phys. Rev. B **69**, 235206 (2004).
[24] B. A. Bernevig and S.-C. Zhang, Phys. Rev. B (to be published).
[25] H. Ebert *et al.*, Phys. Rev. B **53**, 7721 (1996).